ELSEVIER

Donepezil–tacrine hybrid related derivatives as new dual binding site inhibitors of AChE

D. Alonso,[a] I. Dorronsoro,[a] L. Rubio,[a] P. Muñoz,[a] E. García-Palomero,[a] M. Del Monte,[a] A. Bidon-Chanal,[b] M. Orozco,[c] F. J. Luque,[b] A. Castro,[a] M. Medina[a] and A. Martínez[a,*]

[a]Neuropharma, S.A., Avda. de La Industria 52, 28760 Tres Cantos (Madrid), Spain
[b]Departamento de Fisicoquímica, Facultad de Farmacia, Universidad de Barcelona, Avda. Diagonal 643, 08028 Barcelona, Spain
[c]Departamento de Bioquímica y Biología Molecular, Facultad de Química, Universidad de Barcelona, Martí i Franqués 1, 08028 Barcelona, Spain

Abstract—A new series of donepezil–tacrine hybrid related derivatives have been synthesised as dual acetylcholinesterase inhibitors that could bind simultaneously to the peripheral and catalytic sites of the enzyme. These new hybrids combined a tacrine, 6-chlorotacrine or acridine unit as catalytic binding site and indanone (the heterocycle present in donepezil) or phthalimide moiety as peripheral binding site of the enzyme, connected through a different linker tether length. One of the synthesised compounds emerged as a potent and selective AChE inhibitor, which is able to displace propidium in a competition assay. These results seem to confirm the ability of this inhibitor to bind simultaneously to both sites of the enzyme and make it a promising lead for developing disease-modifying drugs for the future treatment of Alzheimer's disease. To gain insight into the molecular determinants that modulate the inhibitory activity of these compounds, a molecular modelling study was performed to explore their binding to the enzyme.
© 2005 Elsevier Ltd. All rights reserved.

1. Introduction

Alzheimer's disease (AD) is the most common form of dementia accounting for about 50–60% of the overall cases of dementia among persons over 65 years of age.[1] It is a progressive, degenerative disorder of the brain characterised by loss of memory and cognition. Brain regions that are associated with higher mental functions, particularly the neocortex and hippocampus, are those most affected by the characteristic pathology of AD.[2] This includes the extracellular deposits of β-amyloid (derived from amyloid precursor protein, APP) in senile plaques,[3,4] intracellular formation of neurofibrillary tangles (containing an abnormally phosphorylated form of a microtubule associated protein, *tau*)[5,6] and the loss of neuronal synapsis and pyramidal neurons.[7] Nevertheless, current treatment approaches in this disease continue being primarily symptomatic, with the major therapeutic strategy based on the cholinergic

hypothesis and specifically on acetylcholinesterase (AChE) inhibition.[8] Accordingly, during the last decade, several cholinergic drugs have been launched on the market, primarily AChE inhibitors indicated for the treatment of mild to moderate AD such as tacrine,[9] donepezil,[10] rivastigmine,[11] or galantamine.[12] More recently, memantine,[13] a moderate affinity NMDA-receptor antagonists, has been approved for the treatment of moderate to severe AD (Fig. 1).

The three-dimensional structure of AChE, as determined by X-ray crystallography, revealed that its active site can apparently be reached only through a deep and narrow 'catalytic gorge'.[14] Inhibitors directed to the active site prevent the binding of the substrate molecule (acetylcholine), or its hydrolysis, either by occupying the site with a high affinity molecule (tacrine)[15] or by reacting irreversibly with the catalytic serine (organophosphates and carbamates).[16] The peripheral site consists of a less well-defined area, located at the entrance of the catalytic gorge. Inhibitors that bind to that site include small molecules, such as propidium,[17,18] and peptide toxins such as fasciculin.[19] Parallel to the development of antidementia drugs, research efforts have been focused, among others, on the therapeutic potential of AChE inhibitors to slow the
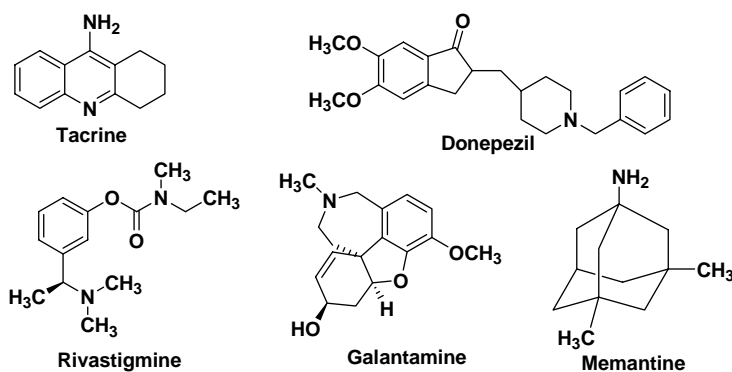
Figure 1. Commercial available drugs for AD treatment.

disorder progression. This fact was based on a range of evidences, which showed that AChE has secondary non-cholinergic functions.[20,21] On the basis of these evidences, it was postulated that AChE binds through its peripheral site to the β-amyloid non-amyloidogenic form acting as a pathological chaperone and inducing a conformational transition to the amyloidogenic conformation with the subsequent amyloid fibril formation.[22] In fact, AChE directly promotes in vitro the assembly of β-amyloid peptide into amyloid fibrils forming stable AChE–β-amyloid complexes.[23] Considering the non-cholinergic aspects of the cholinergic enzyme AChE, their relationship to Alzheimer's hallmarks and the role of the peripheral site of AChE in all these functions, an attractive target for the design of new antidementia drugs emerged.[24] Recent experimental results[25–28] following this approach lead to the synthesis of several chemically diverse structures with potent AChE inhibition and interesting biological profile (Fig. 2). These data corroborate the initial dual site AChE hypothesis[29] and provided a new way to delay the neurodegenerative process.

Continuing our research on catalytic and peripheral binding site inhibitors, that include *N*-benzylpiperidine derivatives of 1,2,4-thiadiazolidinone[30] and tacrine thiadiazolidinone compounds,[31] we present here the synthesis, biological activity and propidium competition assay of novel dual binding site AChE inhibitors. These new

dimeric compounds contain the tacrine heterocycle ring, which is recognised as a catalytic AChE inhibitor and indanone or related heterocycles as responsible for the binding to the peripheral site of the enzyme. These new family of inhibitors could be considered as donepezil–tacrine hybrid related derivatives. To study further the biological profile of these compounds, their butyrylcholinesterase (BChE) inhibitory activity was also evaluated. Finally, to explore the ability to bind the peripheral site of AChE, assays were also performed to explore the capacity to displace propidium binding.

2. Results and discussion

2.1. Chemistry

The synthesis of compounds **7–12** was achieved following a convergent pathway strategy summarized in (Scheme 1). Reaction of tetrahydroacridines **1** or **2** with diaminoalkyl derivatives at reflux afforded the intermediates 9-alkylaminotetrahydroacridines **3a–e** in good yields (60–70%), following a procedure previously known.[32] Compounds **7** and **8** can be prepared through a Mannich-type reaction by treatment of commercially available indanone **4** with paraformaldehyde, and amines **3a** and **3b**. The same reaction using the indadione **5** afforded compound **9** in moderate yield. Coupling reaction of the
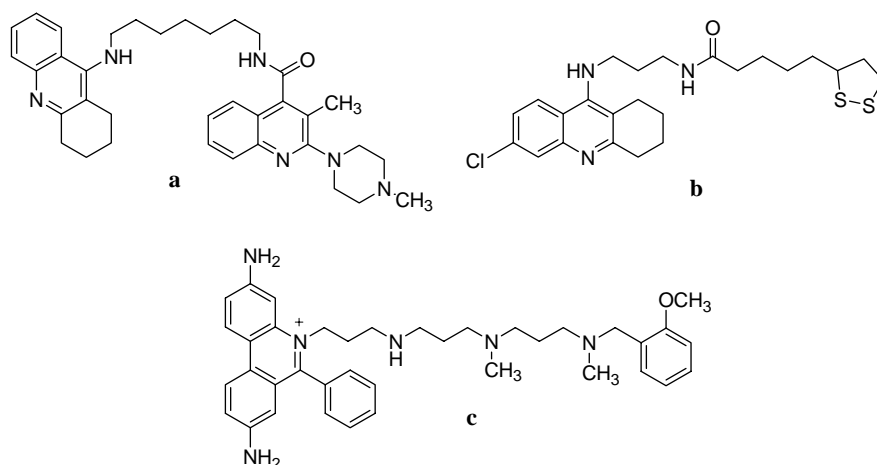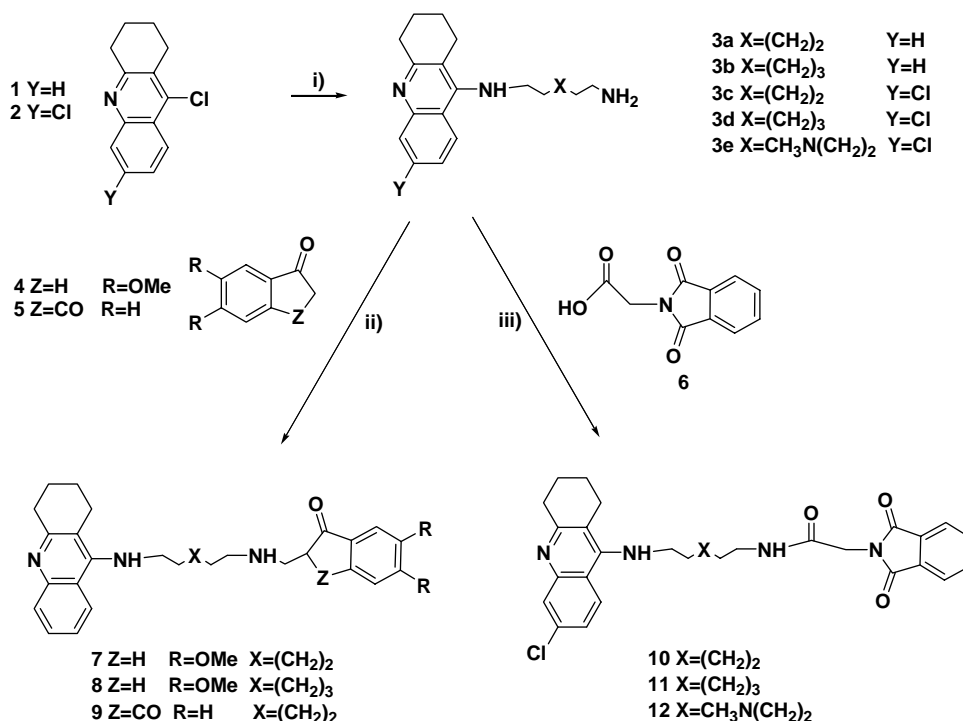

**Figure 2.** Representative dual binding site hybrid AChE inhibitors. **a**, Ref. 26; **b**, Ref. 27 and **c**, Ref. 28.

Scheme 1. Convergent pathway leading to the synthesis of compounds **7–12**. Reagents and conditions: (i) $NH_2(CH_2)_2X(CH_2)_2NH_2$, pentanol, Δ; (ii) HCOH, EtOH/H_2O, HCl, Δ; (iii) CDI, THF, rt.

intermediates **3a–e** with *N*-phthalimide acetic acid **6** in the presence of carbonyldiimidazole (CDI) afforded compounds **10–12** in good yields (Scheme 1). These derivatives **9–12** lack any quiral centre in their chemical structures, which is a great advantage for further pharmaceutical development regarding hybrids **7–8**.
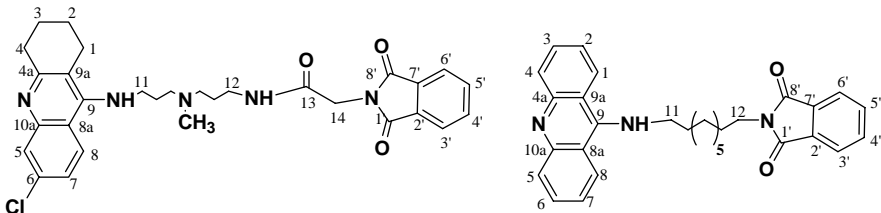
The alkylation of phthalimide with different dibromoalkyl derivatives **13a–d** led to intermediates **15a–d**. Subsequent alkylation of **15a–d** with 9-aminoacridine and 9-aminotetrahydroacridine afforded compounds **17–22** in good yields (Scheme 2).

Unequivocal assignment of ^{1}H and ^{13}C chemical shifts was performed for two representative compounds (**12** and **22**), using bidimensional experiments following HMQC and HMBC sequences. Data are collected in Table 1.
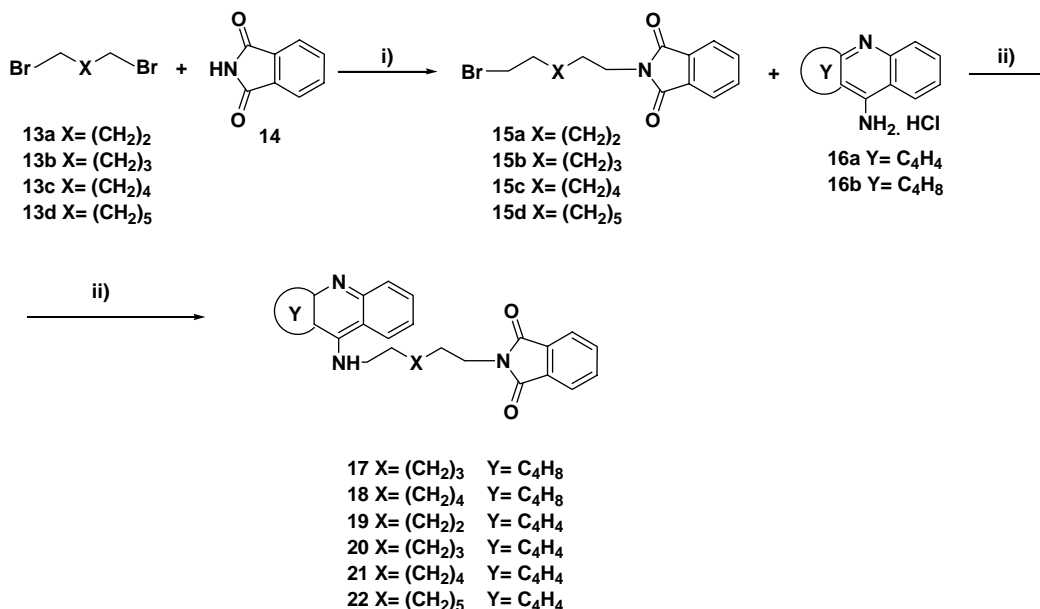
Scheme 2. Synthetic route leading to compounds **17–22**. Reagents and conditions: (i) NaH, DMF, rt; (ii) KOH, DMSO, Δ.

Table 1. Chemical shifts of **12** and **22**

Atom number	Compound **12**		Compound **22**	
	^{1}H (δ ppm) CDCl$_3$, 400 MHz	^{13}C (δ ppm) CDCl$_3$, 100 MHz	^{1}H (δ ppm) CDCl$_3$, 400 MHz	^{13}C (δ ppm) CDCl$_3$, 100 MHz
1	2.58	32.3	8.02	122.5
2	1.80	22.0	7.33	121.3
3	1.80	22.5	7.62	132.7
4	2.90	38.8	8.06	133.6
4a	—	157.3	—	155.4
5	7.90	124.8	8.06	133.6
6	—	135.1	7.62	132.7
7	7.93	124.6	7.33	121.3
8	7.16	124.4	8.02	122.5
8a	—	114.3	—	113.0
9	—	151.8	—	155.4
9a	—	117.0	—	113.0
10a	—	145.4	—	155.4
11	3.22	48.8	3.82	37.6
12	3.48	56.1	3.65	48.6
13	—	167.4	—	—
14	4.21	56.2	—	—
1′	-	166.0	—	168.3
2′		131.6	—	132.0
3′	7.82	123.2	7.80	124.2
4′	7.68	134.0	7.68	134.2
5′	7.68	134.0	7.68	134.2
6′	7.82	123.2	7.80	123.5
7′	—	131.6	—	132.0
8′	—	166.0	—	168.3
N-CH$_3$	2.12	42.3	—	—

2.2. Biological activity and molecular modelling

To evaluate the biological profiles of these heterodimeric compounds for AD, AChE (bovine erythrocytes) and BChE (human plasma) inhibition was assayed in comparison with tacrine and donepezil as reference compounds. The inhibitory potency against AChE and BChE was evaluated by the method of Ellman et al.[33] Compounds **12** and **22** (see Table 2) exhibit an optimum AChE inhibitory activity, as noted in the fact that they are 8-fold and 70-fold more potent than donepezil and tacrine, respectively. Moreover, compounds **12** and **22** showed more than 20-fold selectivity in AChE versus BChE assays (see Table 2). The proper tether length for the linker between the two anchoring groups, 9-aminoacridine and indanone/phthalimide, seemed to be nine (compound **22**) or 10 (compound **12**).

To gain insight into the molecular determinants that modulate the inhibitory activity of these compounds, a molecular modelling study was performed to explore their binding to the enzyme. The position of compounds **12** and **22** with respect to the key residues in the binding site is shown in Figure 3. The tetrahydroacridine/acridine moiety is firmly bound to the catalytic site of AChE, it being stacked against the aromatic rings of Trp84 (average distance between rings of 3.6 and 4.0 Å for compounds **12** and **22**, respectively) and Tyr330 (average distances of 4.3 and 4.9 Å). The aromatic nitrogen of tetrahydroacridine/acridine is hydrogen-bonded to the main-chain carbonyl oxygen of His440 (average N···O distance: 3.0 Å) in **12**. For compound **22** such an interaction was replaced along the simulation by a water-mediated contact (average N···O distance of 4.6 Å along the last ns). Finally, the chlorine atom in **12** occupies a small hydrophobic pocket formed by Trp432, Met436 and Ile439, a feature that has been identified in both modelled[34] and experimental[35] structures of the AChE–huprine Y complex.

With regard to the linker, the most relevant difference between compounds **12** and **22** comes from the presence of the tertiary amine group in the former. Thus, this group forces the tether to reorient along the gorge to form a coulombic interaction with the carboxylate group of Asp72 (average N···O distance: 3.0 Å). Noteworthy, a relevant difference was found in the orientation of the side chain of Asp72 in the AChE complexes with **12** and **22** (see Fig. 3). Finally, the amido

Table 2. Biological activity of donepezil–tacrine hybrids: inhibitory activity on AChE (bovine erythrocyte) and BChE (human serum) and propidium competition assay results

Compound	IC$_{50}$ AChE (nM)	IC$_{50}$ BChE (nM)	Selectivity (AChE/BChE)	Propidium competition (µM)
7	100	50	2	>1000
8	25	0.6	41.6	>1000
9	504	98	5.1	>1000
10	10	220	0.04	10
11	20	660	0.03	100
12	2.8	75	0.04	10
17	3009	10	300	10
18	93	29	3.2	>1000
19	870	7.8	111.5	10
20	1550	711	2.2	100
21	1140	1010	1.1	>1000
22	2.4	90	0.02	1
Tacrine	167	24	6.9	1000
Donepezil	19	930	0.02	1

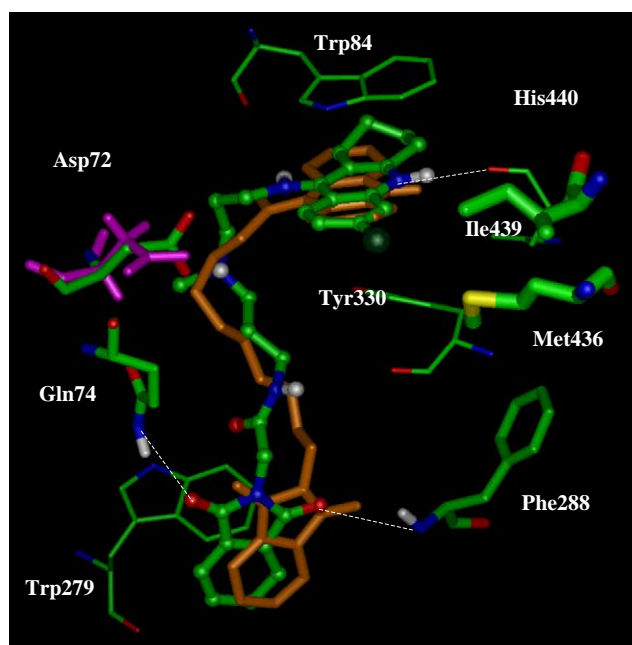Each assay was repeated, at least, three independent times.

Figure 3. Representation of compounds **12** and **22** docked into the binding site of AChE highlighting the protein residues that form the main interactions with the different structural units of the inhibitor. Compound **22** is shown in orange. For the sake of clarity the enzyme residues in the AChE complex with **22** are not shown, but the side chain of Asp72 is shown in magenta. The dotted (white) lines denote hydrogen-bond contacts between the ligand and enzyme residues.

group of compound **12**, which is buried inside the protein gorge, does not, however, make favourable contact with suitable residues of the enzyme.

Finally, the phthalimide ring occupies a similar position in heterodimers **12** and **22** at the peripheral site and remains stacked onto the aromatic ring of Trp279. Moreover, the carbonyl groups of the phthalimide ring form a direct hydrogen-bond contact with the backbone NH group of Phe288 (average O···N distance of 3.1 Å) and a water-mediated interaction with the amide unit of Gln74 (average O···N distance of 4.2 Å).

The preceding findings suggest that the similar AChE inhibitory activity of compounds **12** and **22** (see Table 2) stems not from the existence of a common pattern of interactions, but from a subtle balance of different forces. Compared to the tetrahydroacridine derivative, the larger delocalization of the positive charge in the acridine ring should weaken the stabilizing cation–π interaction at the catalytic site of the enzyme. Binding of compound **12** at the catalytic site should also be favoured by the presence of the chlorine atom, since it is well known that attachment of a chlorine atom at position 6 of tacrine and related compounds leads to largely enhancing the binding affinity.[36] The favourable electrostatic interaction between the tertiary amine in **12** with the side chain of Asp72 should a priori also contribute to the binding of compound **12**. However, this effect must be largely counterbalanced by the desolvation of the protonated amine. In fact, the desolvation cost for compound **12** is estimated to be around 90 kcal/mol larger than for compound **22** according to AM1 semiempirical calculations (determined for the ligand in the bonded conformation) performed with the MST continuum model.[37] Moreover, the formation of the salt bridge between the tertiary amine and Asp72 likely induces steric strain into the linker, thus explaining the need to include an additional methylene group into the tether compared to compound **22**. At this point, it is worth noting that increasing the length of the tether from nine to 10 methylene units decreases the inhibitory potency, as noted in the results determined for compounds **10** and **11** (see Table 2). Finally, the lack of favourable interactions between the amido group in **12** and the enzyme residues should also contribute to decrease the inhibitory potency compared to **22**.

A propidium competition assay was performed to confirm the interaction of the compounds at the peripheral binding site of AChE, since it is known that propidium is a selective ligand for the peripheral site of the enzyme. Moreover, this is an indirect method to predict the potential effect of the inhibitors on β-amyloid aggregation.[38] The fact that the more potent inhibitors **12** and **22** were able to displace propidium in the competition

assay, showing IC_{50} values of 10 and 1 µM, respectively is relevant. The finding that both compounds possess the phthalimide moiety suggests that this chemical unit acts as an efficient ligand for the peripheral site of the enzyme. As it was found for the AChE inhibition, the best binding to the peripheral site of AChE was found for a tether length between the two anchoring groups (9-aminoacridine and phthalimide) of nine units.

In conclusion, the interesting dual binding site AChE profile of compound **22** makes this inhibitor a promising lead for developing disease-modifying drugs for the future treatment of AD.

3. Experimental

3.1. Chemistry

Reagents and solvents were purchased from common commercial suppliers and were used without further purification. Chromatographic separations were performed on silica gel, using either flash chromatography (CC, using Kieselgel 60 Merck of 230–400 mesh) or preparative centrifugal thin layer chromatography (CTLC, on a circular plate coated with a 1 mm layer of Kieselgel 60 PF_{254} gipshaltig, Merck, using a Chromatotron®). Compounds were detected with UV light (254 nm), iodine chamber, or ninhydrin.

Nuclear magnetic resonance spectra were recorded in $CDCl_3$ solutions, using Varian Unity-500, Varian Mercury 400 MHz or Varian 300 MHz spectrometers. Typical spectral parameters for ^1H NMR were: spectral width 10 ppm, pulse width 9 µs (57°) and data size 32 K. The acquisition parameters in decoupled ^{13}C NMR spectra were: spectral width 16 kHz, acquisition time 0.99 s, pulse width 9 µs (57°) and data size 32 K. Chemical shifts are reported in δ values (ppm) relative to internal Me_4Si and J values are reported in hertz. Other experiments, such as heteronuclear single-quantum coherence (HSQC) and heteronuclear multiple bond correlation (HMBC), were obtained in standard conditions. Mass spectra (MS) were obtained by electronic impact (EI) at 70 eV in a Hewlett–Packard 5973 spectrometer (with direct insertion probe) or by electrospray (ES) in a Waters ZQ2000 spectrometer.

3.1.1. General method for the synthesis of compounds 7–9.
To a stirred solution of diamine in a mixture of ethanol/water (3:1), the paraformaldehyde and indanone were added at room temperature. Afterwards the pH was adjusted to 3 with 35% hydrochloric acid and the mixture was refluxed for 24 h. Then, the reaction mixture was cooled to 25 °C and the solvent was removed under vacuum pressure. The resulting residue was treated with K_2CO_3 saturated solution and extracted with methylene chloride. The combined organic extracts were washed with water and dried with anhydrous Na_2SO_4. The solvent was removed under vacuum and the residue was purified by preparative centrifugal thin layer chromatography.

3.1.1.1. 5,6-Dimethoxy-2-{[6-(1,2,3,4-tetrahydro-acridin-9-ylamino)-hexylamino]-methyl}-indan-1-one (7). *Reagents*.
(1,2,3,4-Tetrahydro-acridin-9-yl)-hexane-1,6-diamine (96 mg, 0.32 mmol), ethanol/water 3:1 (3.5 ml), paraformaldehyde (19.2 mg, 0.64 mmol) and indanone (62 mg, 0.32 mmol).

Purification. Silica gel column chromatography using AcOEt/MeOH (10:1)–(3:1) and 0.1% NH_3 saturated. Yellow syrup, yield: 5 mg (1%). ^1H NMR ($CDCl_3$, 300 MHz, δ ppm): 7.99 (d, 2H, $J = 7.0$ Hz), 7.57 (t, 1H, $J = 7$ Hz), 7.54 (t, 1H, $J = 7$ Hz), 7.12 (s, 1H), 6.85 (s, 1H), 3.94 (s, 3H), 3.87 (s, 3H), 3.54 (t, 2H, $J = 7.0$), 3.19 (dd, 1H, $J = 6.83$ Hz, $J = 16.90$ Hz), 3.05 (m, 2H), 2.92 (m, 1H), 2.87 (m, 2H), 2.83 (dd, 1H, $J = 3.40$ Hz, $J = 17.10$ Hz), 2.66 (m, 2H), 2.59 (m, 2H), 1.84 (m, 4H), 1.79 (m, 2H), 1.39 (m, 2H), 1.36 (m, 4H). ^{13}C NMR ($CDCl_3$, 75 MHz, δ ppm): 200.8, 155.30, 151.20, 149.20, 149.04, 129.10, 128.79, 128.30, 123.90, 123.00, 120.10, 119.00, 107.00, 107.38, 105.36, 104.18, 56.25, 56.08, 51.27, 49.73, 49.36, 47.29, 31.64, 31.31, 29.72, 26.98, 26.78, 24.61, 22.89, 22.52. ESI-MS $[M+H^+]^+$ 502.

3.1.1.2. 5,6-Dimethoxy-2-{[7-(1,2,3,4-tetrahydro-acridin-9-ylamino)-heptylamino]-methyl}-indan-1-one (8). *Reagents*.
(1,2,3,4-Tetrahydro-acridin-9-yl)-hexane-1,7-diamine (134 mg, 0.43 mmol), ethanol/water 3:1 (3.5 ml), paraformaldehyde (26 mg, 0.86 mmol) and indanone (83 mg, 0.43 mmol).

Purification. Silica gel column chromatography using AcOEt/MeOH (10:1)–(3:1) and 0.1% NH_3 saturated. Yellow syrup, yield: 7 mg (6.8%). ^1H NMR ($CDCl_3$, 500 MHz, δ ppm): 7.96 (dd, 1H, $J = 6.80$, $J = 1.06$ Hz), 7.94 (dd, 1H, $J = 6.81$, $J = 1.08$ Hz), 7.55 (dt, 1H, $J = 6.82$, $J = 1.07$ Hz), 7.36 (dt, 1H, $J = 6.82$, $J = 1.07$ Hz), 7.14 (s, 1H), 6.86 (s, 1H), 3.95 (s, 3H), 3.89 (s, 3H), 3.50 (t, 2H, $J = 7.25$ Hz), 3.23 (dd, 1H, $J = 6.61$, $J = 16.85$ Hz), 3.08 (m, 2H), 2.89 (t, 2H, $J = 5.97$ Hz), 2.92 (m, 1H), 2.88 (m, 2H), 2.81 (dd, 1H, $J = 3.20$, $J = 17.06$ Hz), 2.69 (m, 2H), 1.91 (m, 4H), 1.67 (m, 2H), 1.48 (m, 2H), 1.33 (m, 4H). ^{13}C NMR ($CDCl_3$, 125 MHz, δ ppm): 200.0, 155.86, 151.35, 149.69, 149.64, 129.60, 128.79, 128.42, 123.92, 123.18, 120.11, 119.06, 107.63, 107.44, 105.36, 104.43, 56.49, 56.328, 51.534, 50.114, 49.70, 47.60, 33.85, 31.92, 31.57, 30.01, 29.47, 27.13, 27.08, 24.92, 23.20, 22.80. ESI-MS $[M+H^+]^+$ 516.

3.1.1.3. 2-[6-(1,2,3,4-Tetrahydro-acridin-9-ylamino)-hexylamino]-indan-1,3-dione (9). *Reagents*.
(1,2,3,4-Tetrahydro-acridin-9-yl)-hexane-1,6-diamine oxalate (339 mg, 0.87 mmol), ethanol/water 3:1 (3.5 ml), paraformaldehyde (26.4 mg, 0.88 mmol) and indan-1,3-dione (129 mg, 0.88 mmol).

Purification. Silica gel column chromatography using AcOEt/MeOH (10:1)–(3:1) and 0.1% NH_3 saturated. Yellow syrup, yield: 17 mg (4.4%). ^1H NMR ($CDCl_3$, 400 MHz, δ ppm): 7.92 (m, 4H), 7.84 (dd, 2H, $J = 6$, $J = 2.8$ Hz), 7.54 (m, 1H), 7.32 (m, 1H), 3.70 (t, 2H, $J = 6.4$), 3.60 (m, 1H), 3.50 (t, 2H, $J = 6.4$ Hz), 3.08 (m, 2H), 2.65 (m, 2H), 31.8–2.0 (m, 4H), 1.80 (m, 2H), 1.70 (m, 2H), 1.45 (m, 4H). ^{13}C NMR ($CDCl_3$, 100 MHz, δ

ppm): 200.0, 159.0, 151.3, 147.1, 140.6, 136.8, 136.1, 130.5, 129.9, 123.6, 123.0, 120.8, 120.4, 53.1, 52.9, 49.3, 48.9, 31.4, 29.8, 26.7, 26.4, 24.7, 22.6, 22.0. ESI-MS [M+H$^+$]$^+$ 457.

3.1.2. General method for the synthesis of compounds 10–12.
Compounds **10–12** have been synthesized following the procedure previously reported in bibliography.[39] 1,1′-Carbonyldiimidazole was added to a solution of isoindol in THF anhydrous was added under N$_2$, and the mixture was stirred for 4 h at room temperature. Then the amine was added and the resulting amber solution was stirred for 20 h. The solvent was evaporated under reduced pressure, water was added and the resulted mixture was extracted with dichloromethane. The combined organic extracts were washed with saturated aqueous NaCl solution and then were dried with anhydrous Na$_2$SO$_4$. The solvent was evaporated under reduced pressure and the residue was purified by silica gel column chromatography using as eluent mixtures of solvents in the proportions indicated for each case.

3.1.2.1. *N*-[6-(6-Chloro-1,2,3,4-tetrahydro-acridin-9-yl-amino)-hexyl]-2-(1,3-dioxo-1,3-dihydroisoindol-2-yl)aceta-mide (10). *Reagents.*
Isoindole acid (160.0 mg, 0.78 mmol), THF anhydrous (10 ml), 1,1′-carbonyldiimidazole (126.47 mg, 0.78 mmol) and 6-chloro-9-(6-aminohexyla-mino)-1,2,3,4-tetrahydroacridine (260 mg, 0.78 mmol).

Purification. Silica gel column chromatography using DCM/MeOH (30:1) and 0.5% NH$_3$ saturated. Yellow solid, yield: 150 mg (37%). ^{1}H NMR (CDCl$_3$, 400 MHz, δ ppm): 7.93 (d, 1H, J = 8.9 Hz), 7.90 (d, 1H, J = 1.9 Hz), 7.82 (dd, 2H, J = 5.0 Hz, J = 2.7 Hz), 7.68 (dd, 2H, J = 5.0 Hz, J = 2.7 Hz), 7.16 (dd, 1H, J = 8.9 Hz, J = 1.9 Hz), 6.64 (m, 1H), 4.30 (s, 2H), 4.21 (m, 1H) 3.50 (m, 2H), 3.30 (c, 2H, J = 7 Hz), 3.05 (m, 2H), 2.65 (m, 2H), 1.80 (m, 4H), 1.68 (q, 2H, J = 7 Hz), 1.55 (q, 2H, J = 7 Hz), 1.40 (m, 4H). ^{13}C NMR (CDCl$_3$, 100 MHz, δ ppm): 167.59, 166.08, 157.63, 151.56, 146.02, 134.88, 134.03, 131.73, 125.44, 124.83, 124.35, 123.32, 117.31, 114.62, 48.90, 40.81, 39.43, 32.80, 31.42, 29.39, 26.23, 24.52, 22.78, 22.28. ESI-MS [M+H$^+$]$^+$ 519.

3.1.2.2. *N*-[7-(6-Chloro-1,2,3,4-tetrahydro-acridin-9-yla-mino)-heptyl]-2-(1,3-dioxo-1,3-dihydroisoindol-2-yl)aceta-mide (11). *Reagents.*
Isoindole acid (100 mg, 0.48 mmol), THF anhydrous (10 ml), 1,1′-carbonyldiimidazole (83.0 mg, 0.51 mmol) and 6-chloro-9-(7-aminoheptyla-mino)-1,2,3,4-tetrahydroacridine (165.5 mg, 0.48 mmol).

Purification. Silica gel column chromatography using DCM/MeOH (30:1) and 0.1% NH$_3$ saturated. Yellow solid, yield: 80 mg (30.8%). ^{1}H NMR (CDCl$_3$, 400 MHz, δ ppm): 7.93 (d, 1H, J = 8.9 Hz), 7.90 (d, 1H, J = 1.9 Hz), 7.82 (dd, 2H, J = 5.0 Hz, J = 2.7 Hz), 7.68 (dd, 2H, J = 5.0 Hz, J = 2.7 Hz), 7.16 (dd, 1H, J = 8.9 Hz, J = 1.9 Hz), 6.64 (m, 1H), 4.30 (s, 2H), 4.21 (m, 1H) 3.48 (m, 2H), 3.26 (c, 2H, J = 7 Hz), 2.90 (m, 2H), 2.65 (m, 2H), 1.80 (m, 4H), 1.68 (q, 2H, J = 7 Hz), 1.50 (q, 2H, J = 7 Hz), 1.30 (m, 6H). ^{13}C NMR (CDCl$_3$, 100 MHz, δ ppm): 167.75, 166.30,

157.24, 152.04, 145.46, 135.11, 134.03, 131.69, 124.86, 124.62, 124.41, 123.27, 117.00, 114.36, 40.50, 39.62, 32.184, 31.27, 29.12, 28.66, 26.56, 26.42, 24.305, 22.56, 22.04. ESI-MS [M+H$^+$]$^+$ 533.

3.1.2.3. *N*-(3-{[3-(6-Chloro-1,2,3,4-tetrahydro-acridin-9-ylamino)-propyl]-methyl-amino}-propyl)-2-(1,3-dioxo-1,3-dihydroisoindol-2-yl)acetamide (12). *Reagents.*
Isoindole acid (71.1 mg, 0.34 mmol), THF anhydrous (10 ml), 1,1′-carbonyldiimidazole (55.1 mg, 0.34 mmol) and N^1-[3-(6-chloro-1,2,3,4-tetrahydro-acridin-9-ylamino)-propyl]-N^1-methyl-propane-1,3-diamine (200 mg, 0.34 mmol).

Purification. Silica gel column chromatography using DCM/MeOH (30:1) and 0.1% NH$_3$ saturated. Yellow solid, yield: 60 mg (31.5%). ^{1}H NMR (CDCl$_3$, 400 MHz, δ ppm): 7.93 (d, 1H, J = 8.9 Hz), 7.90 (d, 1H, J = 1.9 Hz), 7.82 (dd, 2H, J = 5.0 Hz, J = 2.7 Hz), 7.68 (dd, 2H, J = 5.0 Hz, J = 2.7 Hz), 7.16 (dd, 1H, J = 8.9 Hz, J = 1.9 Hz), 6.04 (m, 1H), 4.21 (s, 2H), 4.12 (m, 1H) 3.48 (m, 2H), 3.22 (c, 2H, J = 7 Hz), 2.90 (m, 2H), 2.58 (m, 2H), 2.35 (t, 4H, J = 7 Hz), 2.10 (s, 3H), 1.80 (m, 4H), 1.71 (q, 2H, J = 7 Hz), 1.60 (q, 2H, J = 7 Hz). ^{13}C NMR (CDCl$_3$, 100 MHz, δ ppm): 167.55, 166.02, 157.37, 151.85, 133.99, 131.77, 124.95, 124.16, 123.19, 117,01, 114.41, 56.29, 56.13, 48.88, 42.34, 40.89, 38.89, 32.37, 27.79, 26.15, 24.68, 22.71, 22.15. ESI-MS [M+H$^+$]$^+$ 548.

3.1.3. General method for the synthesis of compounds 17–22.
The bromophthalimide derivates **15a–d** were synthe-sised following the procedure previously reported in bib-liography.[40] 9-Amino-1,2,3,4-tetrahydroacridine was added to a solution of KOH in DMSO under N$_2$, and the mixture was stirred for 4 h at room temperature. Then the brominated derivative was added and the resulting orange solution was stirred for 12 h at room temperature. The DMSO was eliminated by washing with water and extracted with ethyl acetate. The com-bined organic extracts were washed with saturated aque-ous NaCl solution and dried with anhydrous Na$_2$SO$_4$. The solvent was evaporated under reduced pressure and the residue was purified by silica gel column chro-matography using as eluent mixtures of solvents in the proportions indicated for each case.

3.1.3.1. 2-[7-(1,2,3,4-Tetrahydro-acridin-9-ylamino)-hep-tyl]-isoindole-1,3-dione (17). *Reagents.*
9-Amino-1,2,3,4-tetrahydroacridine (100 mg, 0.42 mmol), DMSO (5 ml), KOH (47 mg, 0.8 mmol) and 2-(7-bromo-heptyl)-isoin-dole-1,3-dione (278 mg, 0.8 mmol).

Purification. Silica gel column chromatography using DCM/MeOH (10:1) and 0.5% NH$_3$ saturated. Yellow syrup, yield: 17 mg (5%). ^{1}H NMR (CDCl$_3$, 400 MHz, δ ppm): 8.41 (br s, 1H), 8.12 (d, 1H, J = 8.6 Hz), 7.82 (dd, 2H, J = 5.0 Hz, J = 2.7 Hz), 7.68 (dd, 3H, J = 5.0 Hz, J = 2.7 Hz), 7.43 (t, 1H, J = 8.6 Hz), 3.83 (br s, 2H), 3.65 (t, 2H, J = 7 Hz), 3.25 (br s, 2H), 2.61 (t, 2H, J = 5.8 Hz), 1.97–1.92 (m, 4H), 1.84–1.80 (m, 2H), 1.78–1.72 (m, 2H), 1.47–1.43 (m, 6H). ^{13}C NMR (CDCl$_3$, 100 MHz, δ ppm): 168.5, 166.5, 154.0, 133.8, 132.5, 132.0, 131.2, 128.9, 125.3, 124.1, 123.3, 119.3,

54.6, 49.1, 38.5, 29.7, 29.2, 28.4, 28.2, 26.5, 25.2, 23.4, 22.9, 22.5, 22.1, 21.1, 14.4. ESI-MS [M+H$^+$]$^+$ 443.

3.1.3.2. 2-[8-(1,2,3,4-Tetrahydro-acridin-9-ylamino)-octyl]-isoindole-1,3-dione (18). *Reagents.* 9-Amino-1,2,3,4-tetrahydroacridine (100 mg, 0.42 mmol), DMSO (5 ml), KOH (47 mg, 0.8 mmol) and 2-(8-bromo-octyl)-isoindole-1,3-dione (240 mg, 0.8 mmol).

Purification. Silica gel column chromatography using DCM/MeOH (10:1) and 0.5% NH$_3$ saturated. Yellow syrup, yield: 30 mg (15%). ^{1}H NMR (CDCl$_3$, 400 MHz, δ ppm): 8.43 (br s, 1H), 8.12 (d, 1H, J = 8.6 Hz), 7.82 (dd, 2H, J = 5.0 Hz, J = 2.7 Hz), 7.68 (dd, 3H, J = 5.0 Hz, J = 2.7 Hz), 7.43 (t, 1H, J = 8.6 Hz), 3.83 (br s, 2H), 3.65 (t, 2H, J = 7 Hz), 3.25 (br s, 2H), 2.61 (t, 2H, J = 5.8 Hz), 1.97–1.92 (m, 4H), 1.84–1.80 (m, 2H), 1.78–1.72 (m, 2H), 1.47–1.43 (m, 8H). ^{13}C NMR (CDCl$_3$, 100 MHz, δ ppm): 168.6, 166.2, 154.2, 134.1, 132.6, 132.3, 131.0, 129.0, 125.4, 124.0, 123.3, 119.3, 54.5, 49.0, 38.0, 29.8, 29.2, 28.9, 28.6, 26.7, 25.0, 23.6, 23.0, 22.8, 22.1, 21.0, 14.2. ESI-MS [M+H$^+$]$^+$ 455.

3.1.3.3. 2-[6-(Acridin-9-ylamino)-hexyl]-isoindole-1,3-dione (19). *Reagents.* 9-Amino-acridine (100 mg, 0.42 mmol), DMSO (5 ml), KOH (47 mg, 0.8 mmol) and 2-(6-bromo-hexyl)-isoindole-1,3-dione (240 mg, 0.8 mmol).

Purification. Silica gel column chromatography using DCM/MeOH (10:1) and 0.5% NH$_3$ saturated. Yellow syrup, yield: 30 mg (15%). ^{1}H NMR (CDCl$_3$, 400 MHz, δ ppm): 8.08 (d, 2H, J = 8.6 Hz), 8.02 (d, 2H, J = 8.6 Hz), 7.81 (dd, 2H, J = 5.4 Hz, J = 3.1 Hz), 7.68 (dd, 3H, J = 5.4 Hz, J = 3.1 Hz), 7.59 (t, 2H, J = 6.6 Hz), 7.30 (t, 2H, J = 6.6 Hz) 3.85 (t, 2H, J = 7 Hz), 3.67 (t, 2H, J = 7 Hz), 1.83 (q, 2H, J = 7 Hz), 1.67 (q, 2H, J = 7 Hz), 1.45–1.34 (m, 6H). ^{13}C NMR (CDCl$_3$, 100 MHz, δ ppm): 168.2, 156.3, 133.8, 133.6, 131.9, 128.7, 128.5, 124.7, 123.0, 122.8, 119.3, 111.9, 48.4, 37.68, 29.81, 26.37, 22.81. ESI-MS [M+H$^+$]$^+$ 424.

3.1.3.4. 2-[7-(Acridin-9-ylamino)-heptyl]-isoindole-1,3-dione (20). *Reagents.* 9-Amino-acridine (60 mg, 0.24 mmol), DMSO (5 ml), KOH (27 mg, 0.48 mmol) and 2-(7-bromo-heptyl)-isoindole-1,3-dione (80 mg, 0.24 mmol).

Purification. Silica gel column chromatography using DCM/MeOH (10:1) and 0.1% NH$_3$ saturated. Yellow syrup, yield: 80 mg (74%). ^{1}H NMR (CDCl$_3$, 400 MHz, δ ppm): 8.08 (d, 2H, J = 8.6 Hz), 8.02 (d, 2H, J = 8.6 Hz), 7.81 (dd, 2H, J = 5.4 Hz, J = 3.1 Hz), 7.68 (dd, 3H, J = 5.4 Hz, J = 3.1 Hz), 7.59 (t, 2H, J = 6.6 Hz), 7.30 (t, 2H, J = 6.6 Hz), 3.85 (t, 2H, J = 7 Hz), 3.67 (t, 2H, J = 7 Hz), 1.83 (q, 2H, J = 7 Hz), 1.67 (q, 2H, J = 7 Hz), 1.45–1.34 (m, 6H). ^{13}C NMR (CDCl$_3$, 100 MHz, δ ppm): 168.3, 155.3, 133.8, 133.7, 132.7, 132.0, 124.5, 123.0, 122.9, 121.7, 113.2, 49.0, 37.7, 30.4, 28.6, 28.3, 26.6, 26.5. ESI-MS [M+H$^+$]$^+$ 438.

3.1.3.5. 2-[8-(Acridin-9-ylamino)-octyl]-isoindole-1,3-dione (21). *Reagents.* 9-Amino-acridine (60 mg, 0.24 mmol), DMSO (5 ml), KOH (27 mg, 0.48 mmol)

and 2-(7-bromo-heptyl)-isoindole-1,3-dione (68.64 mg, 0.24 mmol).

Purification. Silica gel column chromatography using DCM/MeOH (10:1) and 0.1% NH$_3$ saturated. Yellow syrup, yield: 20 mg (18.5%). ^{1}H NMR (CDCl$_3$, 400 MHz, δ ppm): 8.06 (d, 2H, J = 8.6 Hz), 8.02 (d, 2H, J = 8.6 Hz), 7.80 (dd, 2H, J = 5.4 Hz, J = 3.1 Hz), 7.68 (dd, 3H, J = 5.4 Hz, J = 3.1 Hz), 7.59 (t, 2H, J = 6.6 Hz), 7.30 (t, 2H, J = 6.6 Hz) 3.82 (t, 2H, J = 7 Hz), 3.65 (t, 2H, J = 7 Hz), 1.83 (q, 2H, J = 7 Hz), 1.68 (q, 2H, J = 7 Hz), 1.45–1.34 (m, 8H) ^{13}C NMR (CDCl$_3$, 100 MHz, δ ppm): 168.3, 155.4, 134.1, 133.7, 132.7, 131.9, 124.6, 123.1, 122.8, 121.7, 113.1, 48.7, 37.6, 30.0, 28.5, 28.1, 26.4, 26.0, 23.2. ESI-MS [M+H$^+$]$^+$ 451.

3.1.3.6. 2-[9-(Acridin-9-ylamino)-nonyl]-isoindole-1,3-dione (22). *Reagents.* 9-Amino-acridine (150 mg, 0.60 mmol), DMSO (10 ml), KOH (67.3 mg, 1.2 mmol) and 2-(9-bromo-nonyl)-isoindole-1,3-dione (68.64 mg, 0.24 mmol).

Purification. Silica gel column chromatography using DCM/MeOH (10:1) and 0.1% NH$_3$ saturated. Yellow syrup, yield: 60 mg (55.5%). ^{1}H NMR (CDCl$_3$, 400 MHz, δ ppm): 8.06 (d, 2H, J = 8.6 Hz), 8.02 (d, 2H, J = 8.6 Hz), 7.80 (dd, 2H, J = 5.4 Hz, J = 3.1 Hz), 7.68 (dd, 3H, J = 5.4 Hz, J = 3.1 Hz), 7.62 (t, 2H, J = 6.6 Hz), 7.33 (t, 2H, J = 6.6 Hz), 3.82 (t, 2H, J = 7 Hz), 3.65 (t, 2H, J = 7 Hz), 1.83 (q, 2H, J = 7 Hz), 1.68 (q, 2H, J = 7 Hz), 1.45–1.34 (m, 10H). ^{13}C NMR (CDCl$_3$, 100 MHz, δ ppm): 168.3, 155.4, 134.2, 133.6, 132.7, 132.0, 124.2, 123.5, 122.5, 121.3, 113.0, 48.6, 37.6, 30.0, 27.5, 28.1, 26.2, 26.0, 23.2, 22.3. ESI-MS [M+H$^+$]$^+$ 451.

3.2. Biological activity and molecular modelling

3.2.1. Inhibition studies on AChE. The AChE inhibition assays were performed using colorimetric method reported by Ellman et al.[33] The assay solution consisted of 0.02 U AChE from bovine erythrocytes, 0.1 M sodium phosphate buffer, pH 8, 0.3 mM 5,5′-dithiobis(2-nitrobenzoic acid) (DTNB, Ellman's reagent) and 0.5 mM acetylthiocholine iodide as the substrate of the enzymatic reaction. The tested compounds were preincubated with the enzyme for 10 min at 30 °C. Enzyme activity was determined by measuring the absorbance at 405 nm for 10 min with a Fluostar optima plate reader (BMG). The reaction rates were compared and the percent of inhibition due to the presence of test compounds was calculated. The IC$_{50}$ is defined as the concentration of each compound that reduces by 50% the enzymatic activity with respect to that without inhibitors. Each reaction was repeated, at least, three independent times.

3.2.2. Inhibition studies on BchE. BChE inhibitory activity was evaluated at 30 °C by the colorimetric method reported by Ellman et al.[33] The assay solution consisted of 0.01 U BChE from human serum, 0.1 M sodium phosphate buffer, pH 8, 0.3 mM DTNB and 0.5 mM butyrylthiocholine iodide as the substrate of the enzymatic reaction. Enzyme activity was determined by

measuring the absorbance at 405 nm for 5 min with a microplate reader Digiscan 340 T. The tested compounds were preincubated with the enzyme for 10 min at 30 °C. The reaction rate was calculated with, at least, triplicate measurements. The IC_{50} is defined as the concentration of compounds that reduces by 50% the enzymatic activity with respect to that without inhibitors.

3.2.3. Propidium competition assay.
Propidium exhibits an increase in fluorescence on binding to AChE peripheral site, making it a useful probe for competitive ligand binding to the enzyme. Fluorescence was measured in a Fluostar optima plate reader (BMG). Measurements were carried out in 100 μl solution volume, in 96-well plates. The buffer used was 1 mM Tris/HCl, pH 8.0, 5 μM AChE which was incubated, for at least 6 h, with the molecules at different concentrations. Twenty micromolar propidium iodide was added 10 min before fluorescence measurement. The excitation wavelength was 485 nm, and that of emission, 620 nm. Each assay was repeated, at least, three different times.

3.2.4. Molecular modelling of compounds 12 and 22.
The simulation system was defined following the protocol used in our previous studies on AChE–ligand complexes,[34,41] which is briefly summarized here. The simulation system was based on the X-ray crystallographic structures of the AChE complexes with tacrine (PDB entry 1ACJ),[42] huprine Y (1E66)[35] and donepezil (1EVE),[43] which were used as templates to position the 9-aminotetrahydroacridine or 9-aminoacridine unit in the catalytic binding site, the linker along the gorge and the phthalimide unit in the peripheral binding site. The enzyme was modelled in its physiologically active form with neutral His440 and deprotonated Glu327, which together with Ser200 form the catalytic triad. The standard ionization state at neutral pH was considered for the rest of ionizable residues with the exception of Asp392 and Glu443, which were neutral, and His471, which was protonated, according to previous numerical titration studies.[15] Finally, Phe330 was replaced by Tyr to reflect the binding site sequence in bovine AChE. The heterodimer was protonated at the tetrahydroacridine or acridine ring, as well as at the tertiary amine in compound **12**. The orientation of the methylene side chain bonded to the tetrahydroacridine or acridine ring was determined by means of geometry optimizations performed at the MP2/6-31G(d) level using Gaussian-03.[44] With regard to the phthalimide moiety, two different starting orientations were initially chosen. In both cases, the phthalimide ring was stacked against Trp279, though they differed by a 180° rotation around the bond linking the indole unit in Trp279. The system was hydrated by centring a sphere of 40 Å of TIP3P[45] water molecules at the inhibitor, paying attention to filling the position of the crystallographic waters inside the binding cavity. The parm98 file of the AMBER force field[46] was used to describe the enzyme. For the inhibitor, the charge distribution of the tetrahydroacridine/acridine ring, linker and phthalimide unit was determined from fitting to the HF/6-31G(d) electrostatic potential using the RESP procedure,[47] and the van der Waals parameters were taken from those defined for related

atoms in AMBER force field. The final model system was partitioned into a mobile region and a rigid region. The former included the inhibitor, all the protein residues containing at least one atom within 15 Å from the inhibitor, and all the water molecules, while the rest of atoms defined the rigid part.

Starting from the two models of the inhibitor bound to the enzyme, the system was energy minimized and equilibrated using the AMBER program.[48] First, all hydrogen atoms were minimized for 2000 steps of steepest descent. Next, the position of water molecules was relaxed for 5000 steps steepest descent plus 3000 steps of conjugate gradient. At this point, the rigid part of the system was kept frozen and the thermalization of the mobile part was started by running four 10 ps molecular dynamics (MD) simulations to increase the temperature up to 298 K. Subsequently, a 6 ns MD simulation was carried out. Only one of the two simulations provided a stable trajectory, as noted in a small positional root-mean square deviation (around 0.8 Å for the backbone atoms in the mobile region with regard to the crystallographic structure) and favourable contacts with the enzyme (see text). The characterisation of the structural features that mediate the binding of the heterodimers to the enzyme was determined by averaging the geometrical parameters for the snapshots (saved every ps) sampled along the last 2 ns of the MD simulation.

References and notes

1. Leifer, B. P. *J. Am. Geriatr. Soc.* **2003**, *51*, 281–288.
2. Shinosaki, K.; Nishikawa, T.; Takeda, M. *Psychiatry Clin. Neurosci.* **2000**, *54*, 611–620.
3. Neve, R. L.; McPhie, D. L.; Chen, Y. *Brain Res.* **2000**, *886*, 54–66.
4. Bayer, T. A.; Wirths, O.; Majtenyi, K.; Hartmann, T.; Multhaup, G.; Beyreuther, K.; Czech, C. *Brain Pathol.* **2001**, *11*, 1–11.
5. Crowther, R. A.; Goedert, M. *J. Struct. Biol.* **2000**, *130*, 271–279.
6. Iqbal, K.; Alonso, A. D.; Gondal, J. A.; Gong, C. X.; Haque, N.; Khatoon, S.; Sengupta, A.; Wang, J. Z.; Grundke-Iqbal, I. *J. Neural Transm. Suppl.* **2000**, *59*, 213–222.
7. Terry, R. D. *J. Neuropathol. Exp. Neurol.* **2000**, *59*, 1118–1119.
8. Tariot, P. N.; Federoff, H. J. *Alzheimer Dis. Assoc. Disord.* **2003**, *17*, 105–113.
9. Kurz, A. *J. Neural Transm. Suppl.* **1998**, *54*, 295–299.
10. Sugimoto, H. *Chem. Rec.* **2001**, *1*, 63–73.
11. Jann, M. W. *Pharmacotherapy* **2000**, *20*, 1–12.
12. Zarotsky, V.; Sramek, J. J.; Cutler, N. R. *Am. J. Health Syst. Pharm.* **2003**, *60*, 446–452.
13. Reisberg, B.; Doody, R.; Stöffler, A.; Schmitt, F.; Ferris, S.; Möbius, H. J. *N. Engl. J. Med.* **2003**, *348*, 1333–1341.
14. Sussman, J. L.; Harel, M.; Silman, I. *Chem. Biol. Interact.* **1993**, *87*, 187–197.
15. Wlodek, S. T.; Antosiewicz, J.; McCammon, J. A.; Stratsma, T. P.; Gilson, M. K.; Briggs, J. M.; Humblet, C.; Sussman, J. L. *Biopolymers* **1996**, *38*, 109–117.
16. Bartolucci, C.; Perola, E.; Cellai, L.; Brufani, M.; Lamba, D. *Biochemistry* **1999**, *38*, 5714–5719.
17. Szegletes, T.; Mallender, W. D.; Thomas, P. J.; Rosenberry, T. L. *Biochemistry* **1999**, *38*, 122–133.

18. Rosenberry, T. L.; Mallender, W. D.; Thomas, P. J.; Szegletes, T. *Chem. Biol. Interact.* **1999**, *119–120*, 85–97.

19. Harel, M.; Kleywegt, G. J.; Ravelli, R. B.; Silman, I.; Sussman, J. L. *Structure* **1995**, *3*, 1355–1366.

20. Soreq, H.; Seidman, S. *Nat. Rev. Neurosci.* **2001**, *2*, 8–17.

21. Blasina, M. F.; Faria, A. C.; Gardino, P. F.; Hokoc, J. N.; Almeida, O. M.; Mello, F. G.; Arruti, C.; Dajas, F. *Cell Tissue Res.* **2000**, *299*, 173–184.

22. Campos, E. O.; Alvarez, A.; Inestrosa, N. C. *Neurochem. Res.* **1998**, *23*, 135–140.

23. Inestrosa, N. C.; Alvarez, A.; Calderon, F. *Mol. Psychiatry* **1996**, *1*, 359–361.

24. Castro, A.; Martinez, A. *Mini-Rev. Med. Chem.* **2001**, *1*, 267–272.

25. Tumiatti, V.; Andrisano, V.; Banzi, R.; Bartolini, M.; Rosini, M.; Melchiorre, C. *J. Med. Chem.* **2004**, *47*, 6490–6498.

26. Cappelli, A.; Gallelli, A.; Manini, M.; Anzini, M.; Mennuni, L.; Makovec, F.; Menziani, C.; Alcaro, S.; Ortuso, F.; Vomero, S. *J. Med. Chem.* **2005**, *48*, 3564–3575.

27. Rosini, M.; Andrisano, V.; Bartolini, M.; Bolognesi, M.; Hrelia, P.; Minarini, A.; Tarozzi, A.; Melchiorre, C. *J. Med. Chem.* **2005**, *48*, 360–363.

28. Bolognesi, M.; Andrisano, V.; Bartolini, M.; Banzi, R.; Melchiorre, C. *J. Med. Chem.* **2005**, *48*, 24–27.

29. Dorronsoro, I.; Castro, A.; Martinez, A. *Expert Opin. Ther. Patents* **2003**, *13*, 1725–1732.

30. Martinez, A.; Fernandez, E.; Castro, A.; Conde, S.; Rodríguez-Franco, I.; Baños, J. B.; Badia, A. *Eur. J. Med. Chem.* **2000**, *35*, 913–922.

31. Dorronsoro, I.; Alonso, D.; Castro, A.; Del Monte, M.; Garcia-Palomero, E.; Martinez, A. *Arch. Pharm. Pharm. Med. Res.* **2005**, *338*, 18–23.

32. Carlier, P. R.; Chow, E. S.-H.; Han, Y.; Liu, J.; El Yazal, J.; Pang, Y.-P. *J. Med. Chem.* **1999**, *42*, 4225–4231.

33. Ellman, G. L.; Courtney, K. D.; Andres, B.; Featherstone, R. M. *Biochem. Pharmacol.* **1961**, *7*, 88–95.

34. Camps, P.; El Achab, R.; Morral, J.; Muñoz-Torrero, D.; Badia, A.; Baños, J. E.; Vivas, N. M.; Barril, X.; Orozco, M.; Luque, F. J. *J. Med. Chem.* **2000**, *43*, 4657–4666.

35. Dvir, H.; Wong, D. M.; Harel, M.; Barril, X.; Orozco, M.; Luque, F. J.; Muñoz-Torrero, D.; Camps, P.; Rosenberry, T. L.; Silman, I.; Sussman, J. L. *Biochemistry* **2002**, *41*, 2970–2981.

36. Barril, X.; Kalko, S. G.; Orozco, M.; Luque, F. J. *Mini-Rev. Med. Chem.* **2002**, *2*, 27–36.

37. Curutchet, C.; Salichs, A.; Barril, X.; Orozco, M.; Luque, F. J. *J. Comput. Chem.* **2002**, *24*, 32–45.

38. Taylor, P.; Lappi, S. *Biochemistry* **1975**, *14*, 1989–1997.

39. Padwa, A.; Harring, S. R.; Hertzog, D. L.; Nadlet, W. R. *Synthesis* **1994**, *9*, 993–1004.

40. Donahoe, H.; Seiwald, R.; Newman, M.; Kimura, K. *J. Org. Chem.* **1957**, *22*, 68–70.

41. Barril, X.; Orozco, M.; Luque, F. J. *J. Med. Chem.* **1999**, *42*, 5110–5119.

42. Sussman, J. L.; Harel, M.; Frolow, F.; Oefner, C.; Goldman, A.; Toker, L.; Silman, I. *Science* **1991**, *253*, 872–879.

43. Kryger, G.; Silman, I.; Sussman, J. L. *Structure* **1999**, *7*, 297–307.

44. Frisch, M. J.; Trucks, G. W.; Schlegel, H. B.; Scuseria, G. E.; Robb, M. A.; Cheeseman, J. R.; Montgomery, J. A., Jr.; Vreven, T.; Kudin, K. N.; Burant, J. C.; Millam, J. M.; Iyengar, S. S.; Tomasi, J.; Barone, V.; Mennucci, B.; Cossi, M.; Scalmani, G.; Rega, N.; Petersson, G. A.; Nakatsuji, H.; Hada, M.; Ehara, M.; Toyota, K.; Fukuda, R.; Hasegawa, J.; Ishida, M.; Nakajima, T.; Honda, Y.; Kitao, O.; Nakai, H.; Klene, M.; Li, X.; Knox, J. E.; Hratchian, H. P.; Cross, J. B.; Adamo, C.; Jaramillo, J.; Gomperts, R.; Stratmann, R. E.; Yazyev, O.; Austin, A. J.; Cammi, R.; Pomelli, C.; Ochterski, J. W.; Ayala, P. Y.; Morokuma, K.; Voth, G. A.; Salvador, P.; Dannenberg, J. J.; Zakrzewski, V. G.; Dapprich, S.; Daniels, A. D.; Strain, M. C.; Farkas, O.; Malick, D. K.; Rabuck, A. D.; Raghavachari, K.; Foresman, J. B.; Ortiz, J. V.; Cui, Q.; Baboul, A. G.; Clifford, S.; Cioslowski, J.; Stefanov, B. B.; Liu, G.; Liashenko, A.; Piskorz, P.; Komaromi, I.; Martin, R. L.; Fox, D. J.; Keith, T.; Al-Laham, M. A.; Peng, C. Y.; Nanayakkara, A.; Hallacombe, M.; Gill, P. M. W.; Johnson, B.; Chen, W.; Wong, M. W.; Gonzalez, C.; Pople, J. A. Gaussian 03, Revision B.04, Gaussian, Inc., Pittsburgh, PA, 2003.

45. Jorgensen, W. L.; Chandrasekhar, J.; Madura, J. D.; Impey, R. W.; Klein, M. L. *J. Chem. Phys.* **1983**, *79*, 926–935.

46. Cornell, W. D.; Cieplak, P.; Bayly, C. I.; Gould, I. R.; Merz, K. M.; Ferguson, D. M.; Spellmeyer, D. C.; Fox, T.; Caldwell, J. W.; Kollman, P. A. *J. Am. Chem. Soc.* **1995**, *117*, 5719–5797.

47. Bayly, C. I.; Cieplak, P.; Cornell, W. D.; Kollman, P. A. *J. Phys. Chem.* **1993**, *97*, 10269–10280.

48. Case, D. A.; Darden, T. A.; Cheatham, T. E.; Pearlman, D. A.; Simmerling, C. L.; Wang, J.; Duke, R. E.; Luo, R.; Merz, K. M.; Pearlman, D. A.; Crowley, M.; Brozell, S.; Tsui, V.; Gohlke, H.; Mongan, J.; Hornak, V.; Cui, G.; Beroza, P.; Schafmeister, P.; Caldwell, J. W.; Ross, W. S.; Kollman, P. A. AMBER8. University of California, San Francisco, 2004.